NMR Spectroscopy

DOI: 10.1002/anie.201101739

Structural Discrimination in Small Molecules by Accurate Measurement of Long-Range Proton–Carbon NMR Residual Dipolar Couplings**

Pablo Trigo-Mouriño, Armando Navarro-Vázquez, Jinfa Ying, Roberto R. Gil, and Ad Bax**

Although residual dipolar couplings (RDCs) are widely used in macromolecular structural studies in relation to NMR spectroscopic experiments,[1] they are also proving to be very powerful for the constitutional,[2] configurational,[3–9] and conformational analysis[10,11] of small molecules. Before RDCs were available, the determination of the 3D structure of small molecules by NMR experiments in solution was principally achieved on the basis of parameters such as NOE interactions and ^3J coupling constants. However, if the chain of short-range spin–spin interactions is "interrupted", for example by a magnetically inactive linker, there often is no way to determine the relative configuration of the two disconnected molecular fragments by conventional NMR analysis. This situation is not uncommon, and many unsolved structures are "waiting" for a better method that will permit their identification. Residual dipolar couplings can provide the solution for such problems as they can provide information on the relative configuration of remotely located stereogenic centers.

[*] P. Trigo-Mouriño, R. R. Gil
Department of Chemistry, Carnegie Mellon University
4400 Fifth Ave, Pittsburgh, PA 15213 (USA)
E-mail: rgil@andrew.cmu.edu

P. Trigo-Mouriño, A. Navarro-Vázquez
Departamento de Química Orgánica, Universidade de Vigo
36310 Vigo (Spain)

J. Ying, A. Bax
Laboratory of Chemical Physics, National Institute of Diabetes and Digestive and Kidney Diseases, National Institutes of Health
Bethesda, MD 20892 (USA)
E-mail: bax@nih.gov

[**] NMR instrumentation at CMU is partially supported by the NSF (CHE-0130903). A.N. thanks Centro de Supercomputación de Galicia (CESGA) for computer time, Xunta de Galicia/FEDER (Consellería de Educación 2009/071) for financial support, the Spanish Government for a research grant (CTQ2007-65310), and a "Ramón y Cajal" research contract. We thank Dr. N. V. Tsarevsky from Southern Methodist University (Dallas, TX) for PMMA gels and Dr. V. E. Nicotra from Córdoba National University (Córdoba, Argentina) for the authentic sample of 10-epi (**1**). This work was supported by the Intramural Research Program of the NIDDK, the NIH, and the Intramural AIDS-Targeted Antiviral Program of the Office of the Director, NIH.

Supporting information for this article, including general and specific experimental procedures for the NMR measurements, preparation of alignment, experimental and computed RDCs values for all 10-epi (**1**) isomers, as well as molecular mechanics and DFT computational details, is available on the WWW under http://dx.doi.org/10.1002/anie.201101739.

After the initial introduction of water-compatible weak-alignment media for studies of biomolecular compounds, development of new alignment media compatible with organic solvents has extended RDC technology to analysis of organic compounds. These alignment methods include liquid-crystalline phases such as those formed by homopolypeptides in $CDCl_3$,[7,12–14] and a variety of different polymer gels that swell in a broad range of organic solvents.[15] In addition, devices that reversibly stretch[16] and compress[17] such swollen polymer gels have been recently developed, thus permitting the collection of rapidly tunable RDC values.

Nearly all of the studies published thus far on the application of RDCs to the constitutional, configurational, and conformational analysis of small molecules, mainly natural products, involved the use of only one-bond ^{1}H–^{13}C RDCs ($^1D_{CH}$) at natural abundance. These $^1D_{CH}$ values are relatively easy to measure, either from F_2 or F_1 cross-sections through ^{1}H-coupled HSQC spectra, where RDCs add to the observed $^1J_{CH}$ splitting: $^nT_{CH} = {}^nJ_{CH} + {}^nD_{CH}$, where $^nT_{CH}$ is the total coupling between a proton and a ^{13}C located n bonds away. With $^1J_{CH}$ coupling constants being large and well resolved, an additional $^1D_{CH}$ contribution to the splitting upon inducing weak alignment is easily quantified from the change in the splitting. These studies have shown that $^1D_{CH}$ couplings can suffice to solve configurational problems in small rigid or semirigid molecules. However, there are many situations in which it is desirable or essential to have more independent RDCs, such as for: 1) molecules where the individual fragments containing the stereogenic centers have too few CH bonds, or where the CH bonds are close to being parallel to one another, such that their RDC values are not independent;[9,18] or 2) rigid or semirigid molecules with multiple unknown stereogenic centers, in which different configurations and/or conformations fit equally well to the experimental set of $^1D_{CH}$ data. Such cases are actually quite common but, as we will demonstrate here, measurement of two- and three-bond RDCs ($^2D_{CH}$ and $^3D_{CH}$) is readily feasible and can solve such problems.

Dipolar couplings scale with $1/r^3$, where r is the internuclear distance; therefore $^2D_{CH}$ and $^3D_{CH}$ couplings cover a range that is about an order of magnitude smaller than $^1D_{CH}$ values requiring a measurement precision that is much higher than for $^1D_{CH}$ values. Although the value of long-range D_{CH} couplings is well recognized, and methods for their measurement have been described,[9,18] their accurate measurement has proved challenging,[15,19] therefore limiting their general application.

Herein, we present a simple and effective NMR experiment that allows the measurement of long-range CH RDCs at very high precision, and describe its application to the configuration determination of a sesquiterpene lactone with five stereogenic centers. The new pulse sequence is shown in Figure 1 and it integrates the conceptual simplicity of the selective ^{1}H-flip experiment[20] into the widely used ^{1}H-detected HSQC experiment, which is enhanced by gradient selection of coherence pathways for sensitivity enhancement and suppression of artifacts.[21] Further suppression of artifacts and a minor sensitivity enhancement, resulting from positive ^{1}H–^{1}H NOE interactions, is accomplished by generating a mostly saturated state for ^{12}C-attached protons by inverting them through a bilinear rotation and subsequent recovery delay Δ,[22] prior to the start of the actual selective *J*-scaled (SJS) HSQC experiment. The actual gradient-enhanced SJS-HSQC experiment starts at the end of the Δ period with an INEPT transfer of ^{1}H magnetization to ^{13}C, and uses τ and τ' delays that are optimized for simultaneous detection of methine, methylene, and methyl signals.[23] The evolution period in this experiment is preceded by a selective *J*-dephasing period, of duration κt_1, which enhances by a factor κ the F_1 dimension J_{CH}-splitting to the proton selectively inverted by the 180°$_{\phi 2}$ pulse.[24] Importantly, effects of static field inhomogeneity, which can be problematic in aligned samples, are refocused at the end of the κt_1 period, and do not impact resolution of the doublet splitting. Also, as in the original selective ^{1}H-flip experiment, only a single proton is inverted per experiment, thus resulting in doublets for each ^{13}C atom coupled to this proton (triplets or quartets if equivalent methylene or methyl protons are selected for inversion). This method results in strikingly simple spectra, which for a doublet splitting only decrease by about two-fold in sensitivity relative to the optimized gradient-enhanced HSQC experiment. The use of a large scaling factor κ ($\kappa = 20$ in our experiments), affords high resolution of the $^nJ_{CH}$ doublets with a limited number of t_1 increments, thus allowing rapid probing of couplings to different protons in consecutive HSQC experiments.

For technical reasons, the experiment is coded with two 180° pulses during the time where ^{13}C magnetization evolves. This makes it possible to use adiabatic pulses for refocusing purposes, as these compensate each other's phase imperfections.[25] Use of the gradient-enhanced pulse scheme to transfer magnetization from ^{13}C back to ^{1}H, to first order, leaves unchanged the spin state of protons not attached to a ^{13}C atom (neglecting pulse imperfections and ^{1}H–^{1}H dephasing and relaxation during the short $2\tau + 2\tau' + 2\delta$ period). Therefore, when a proton, ^1H_A, is selected by the 180°$_{\phi 2}$ ^{1}H pulse between ^{13}C evolution and ^{1}H detection, this results in an E.COSY type multiplet,[26] where the ^{13}C splitting for a given ^1H_B–$^{13}C_B$ correlation corresponds to J_{HA-CB}, and the F_2 displacement of the two doublet components equals J_{HA-HB}. The direction of the relative displacement then contains the relative sign of the J_{HA-CB} and J_{HA-HB} coupling constants (Figure 2B,C).

The experiment described above was demonstrated for 10-epi-8-deoxycumambrin B (**1,** Figure 3), below simply referred to as 10-epi, a biologically relevant sesquiterpene lactone (SQL).[27] The natural absolute configuration at C7 in SQL's isolated from Compositae plants is always *S*.[28]

10-Epi (**1**) was aligned in a PMMA gel swollen in $CDCl_3$ using the previously described, reversible compression/relaxation method.[17] The $^1D_{CH}$ couplings were measured for C1–H1, C3–H3, C5–H5, C6–H6, and C7–H7 using F_1-dimension ^{1}H-coupled HSQC experiments. The $^1D_{CH}$ couplings for C13–H13a, C13–H13b, as well as the two-bond ^{1}H–^{1}H RDC ($^2D_{HH}$) for the pair H13a–H13b were measured using a *J*-modulated HMQC-type experiment.[29] For the methylene groups of C2, C8, and C9, measurement of accurate $^1D_{CH}$ and $^2D_{HH}$ couplings was prevented by very extensive $^nD_{HH}$ splittings to other, passive protons. Instead, the sum of the two $^1D_{CH}$ couplings for each of these methylene groups was determined from the F_1-dimension ^{1}H-coupled HSQC, as were the $^1D_{CH}$ couplings for methyl groups at C14 and C15.

Use of the SJS-HSQC experiment, and selecting only four proton resonances (H2α, H5, H6, and the overlapping H3/H13b) added 15 more RDCs (see the Supporting Information). For example, selective inversion of H5 allowed measurement of its couplings to C1, C2, C3, C6, C7, and C15 (Figure 2A). Although, at first sight, it appears prerequisite for selective inversion of a given proton resonance, H_A, that is well isolated from other resonances in the ^{1}H spectrum, in practice this requirement does not apply as long as protons overlapping or resonating in the vicinity of H_A do not have a long-range scalar or dipolar coupling to the ^{13}C atom whose coupling to H_A needs to be measured in the 2D spectrum. For example, the nearly overlapping resonances of H3 and H13b, located on opposite ends of 10-epi, were inverted with a single pulse in the same

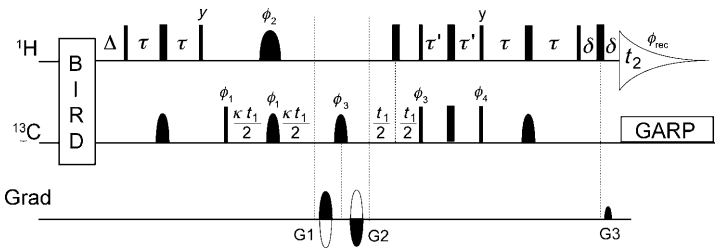

Figure 1. Pulse sequence of the SJS-HSQC experiment for selective measurement of remote $^nJ_{C-H}$ and $^nJ_{H-H}$ coupling constants. Narrow- and wide-filled bars represent 90° and 180° pulses, respectively. All the shaped ^{13}C pulses are of the adiabatic hyperbolic secant type, with a duration of 500 μs (at 187.9 MHz ^{13}C frequency), centered at $\delta = 73$ ppm. The shaped ^{1}H pulse (6.5–25 ms at 747 MHz ^{1}H frequency) has the profile of the center lobe of a $\sin(x)/x$ function, and selectively inverts the resonance of individual proton(s) whose long-range coupling constants are to be measured. The BIRD pulse cluster [$90_x(^1H)$-2τ-$180_x(^1H/^{13}C)$-2τ-$90_{-x}(^1H)$] helps to suppress signals and t_1 noise from protons attached to ^{12}C atoms.[22] Unmarked pulses have phase *x*; $\phi_1 = x$, $-x$; $\phi_2 = 4(x)$, $4(-x)$; $\phi_3 = 2(x)$, $2(-x)$; $\phi_4 = 2(y)$, $2(-y)$; and $\phi_{rec} = x, -x, -x, x$. Quadrature detection in the ^{13}C dimension is achieved using the echo-antiecho approach by inverting ϕ_4 as well as the G1 and G2 gradient pulses for every other t_1 increment.[21] Gradient pulses are sine bell shaped with durations of 600, 400, and 251 μs and peak power of 24, −24, and 24 G cm^{-1} in the *x*- and *y*-directions, and 28, −28, and 28 G cm^{-1} in the *z*-direction for G1, G2, and G3, respectively. Delays: $\tau = 1.61$ ms; $\tau' = 0.89$ ms; $\delta = 459$ μs; and $\Delta = 375$ ms. The $^nJ_{CH}$ scaling factor κ is 20.

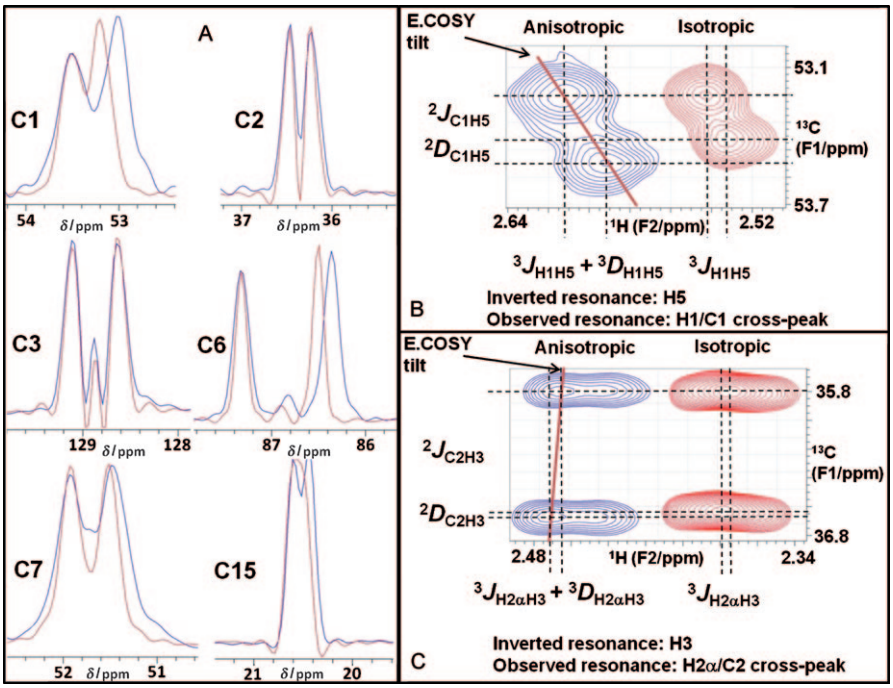

Figure 2. Extraction of RDC values from SJS-HSQC spectra. A) Superimposed plots of F_1 slices through the C1, C2, C5, C3, C6, and C15 cross-peaks of the isotropic (red) and anisotropic (blue) SJS-HSQC spectra, where H5 is selectively inverted. The downfield doublet components are aligned to more clearly show the change in splitting upon alignment (blue) caused by the RDC to H5. B) Side-by-side comparison of the H1/C1 cross-peak of the isotropic (red) and anisotropic (blue) spectra when H5 was selectively inverted. C) Same for the H2α/C2 cross-peak when H3 was selectively inverted. The E.COSY patterns[34] shown indicates the $^3J_{HH}$ and $^2J_{CH}$ values have opposite sign in (B) and the same sign in (C). With $^3J_{HH}$ being positive $^2J_{C_1H_5}$ is negative and $^2J_{C_2H_3}$ is positive. The unusual positive sign of $^2J_{C_2H_3}$ is as expected for $^2J_{CH}$ coupling constants in terminal geminal olefinic C–H pairs.[30]

experiment, thus giving couplings between H13b and C7, as well as between H3 and C1, C2, C5, and C15. The measurement needs to be carried out on isotropic and aligned states of the sample, with the isotropic $^2J_{CH}$ and $^3J_{CH}$ couplings being configurationally and conformationally informative too.[30]

The multiplet pattern in the 2D spectrum is particularly simple and clean (Figure 2), and allows direct reading of the couplings from the spectrum. For the isotropic measurements, $^3J_{CH}$ is known to either be positive or very close to zero; the sign of $^2J_{CB-HA}$ can be established from the known positive value of $^3J_{HB-HA}$, by using the above mentioned E.COSY effect (see legend to Figure 2). Regarding the sign of $^nJ_{CH}+{}^nD_{CH}$, this often follows from the sign of $^nJ_{CH}$ as oppositely signed $^nJ_{CH}$ and $^nD_{CH}$ would require $^nD_{CH}$ values outside of the feasible range. However, when $|{}^nJ_{CH}|$ is small, both possible solutions may need to be explored when fitting the RDCs to the structure, or the measurement needs to be repeated at smaller (or larger) alignment strength.

For well-resolved doublets, an approximate lower limit for the precision at which the corresponding $^nD_{CH}$ coupling can be determined is given by LW/SN, where LW is the line width (down-scaled by κ) and SN the signal-to-noise ratio in the weaker of the two 2D spectra (usually the one acquired for the aligned sample).[31] For 10-epi, κ-scaled ^{13}C line widths are in the 1–1.5 Hz range, with SN varying between 20 and 100. For the well-resolved doublets, measurement errors in $^nD_{CH}$ couplings therefore fall in the 0.01–0.1 Hz range, and even after accounting for the large r_{CH} internuclear distance (which amplify the importance of such errors by r_{CH}^3 when interpreting $^nD_{CH}$ in terms of vector orientation) the accuracies of such measurements are more than sufficient to allow discrimination of different isomers. For doublets that cannot be uniquely resolved in the ^{13}C dimension alone, the E.COSY pattern frequently allows measurement of the sign and magnitude of the coupling (e.g. $^2J_{H6C5}$, see Figure S7 in the Supporting Information), albeit at lower precision.

For several ^{13}C nuclei, for example, C7 in Figure 2 A, an increase in line width is observed in the aligned state, which originates from the increased number of protons interacting with any given ^{13}C atom in the aligned state through residual dipolar coupling, combined with the finite lifetime (T_1) of the spin states of these protons. When either the $^nJ_{CH}$ or $^nJ_{CH}+{}^nD_{CH}$ splitting is not resolved as a doublet, there is increased uncertainty regarding the exact value and sign of the coupling (see for example, Table S1 in the Supporting Information). In addition, there can be some uncertainty in the precise internuclear distance of the long-range coupled ^{13}C–^{1}H spin pair, either as a result of inaccuracies in the coordinates of the models determined by DFT (see below) or from non-linear effects related to bending and stretching motions. Typically, the impact on computed $^nD_{CH}$ values will be less than 10%, but this can be comparable to the measurement error and then may need to be taken into account.

The configurational and conformational space of the structure of 10-epi (**1**) was explored by means of molecular mechanics and DFT calculations—maintaining the configuration at C7 as *S* in all 16 possible diastereomers at C1, C5, C6, and C10 (see the Supporting Information for details). Each structure was named after the configuration at carbons C1, C5, C6, C7, and C10 (e.g. **1** was named *RRSSS*).

As is normally done with small rigid or semirigid molecules, the correct configuration is selected from a complete set of structures by best fitting of the RDC data to each possible isomer.[3–9] For this purpose, we used singular value decomposition (SVD),[32] as implemented in an in-house version of the program MSpin.[33]

To show the impact of long-range RDCs on structural discrimination, two different scenarios were evaluated. Initial fits, including individual experimental errors, were performed

using only the one-bond RDCs and the additional H13a–H13b RDC, but excluding the *D* constants from CH_2 sum splitting for C2, C8, and C9, and methyl groups 14 and 15 (Scenario 1). For those structures containing more than one conformation (*RSSSR*, *RSSSS*, *SRRSS*, *SRSSR*) a population-weighted single tensor SVD fit was performed after superimposition of structures to maximize decoupling between conformational and overall rotational movements.[10,35] The Cornilescu quality factor, *Q*, was used to quantify the structural discrimination of the fits.[36] Three isomers were found to fit well with *Q* factors below 0.1: 10-epi *RRSSS* ($Q = 0.039$), *SRSSS* ($Q = 0.057$), and *RRSSR* ($Q = 0.099$; Figure 3, white bars). When the additional 15 long-range RDCs were added to the SVD fits, the *Q* factor for 10-epi (the correct structure) slightly increased ($Q = 0.060$), as expected when fitting more experimentally observed values with the same number (five) of adjustable parameters. Notably, however, the wrong structures *SRSSS* and *RRSSR* showed much larger deterioration in fit quality ($Q = 0.228$ and $Q = 0.128$, respectively; Figure 3, black bars). In a second scenario, when the CH_2 sum-splitting for C2, C8, and C9, as well as the methyl groups RDCs were included in the fitting, and no long-range RDCs were used, the *Q* factor for 10-epi increased to 0.078, while the *Q* factors for *SRSSS* and *RRSSR* increased to 0.146 and 0.155, respectively.

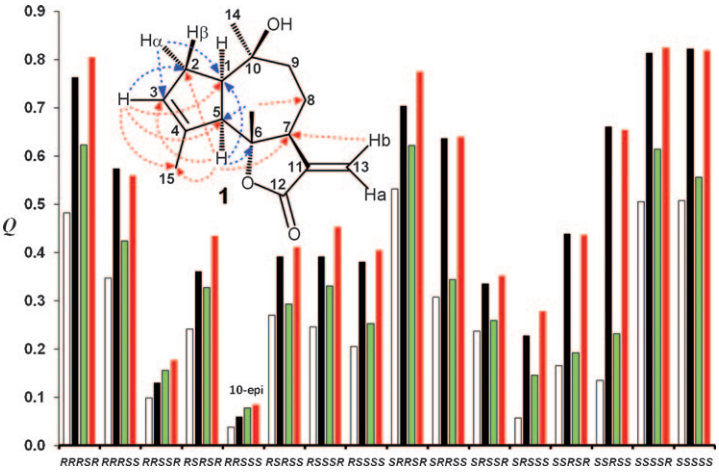

Figure 3. Comparison of *Q* factors obtained from the SVD fits of the experimental RDC data to each possible configuration of **1**: Scenario 1 without long-range couplings (white bars) and after addition of long-range couplings (black bars); Scenario 2 without long-range couplings (green bars) and after addition of long-range. The arrows in the structure represent the distance vectors of the long-range ^1H–^{13}C RDCs ($^2D_{CH}$ in blue, $^3D_{CH}$ in red) measured with the SJS-HSQC experiment.

When long-range RDCs are added to the fitting in scenario 2, it is noteworthy that the *Q* factor for 10-epi barely changed (to $Q = 0.085$; Figure 3, red versus green bars). Meanwhile the *Q* factors from the wrong configurations all increased significantly (e.g. *SRRSS*, *SSRSR*, and *SSRSS*). The complete set of *Q* factors is listed in the Supporting Information.

Alternatively, if only one-bond SVD fits (Scenario 1) are performed and the long-range couplings are predicted for each fit, the comparison of predicted with back-calculated long-range couplings proves equally revealing for discriminating 10-epi from *SRSSS* (see Figure S10 in the Supporting Information).

In conclusion, the SJS-HSQC experiment gives accurate long-range CH RDCs ($^2D_{CH}$ and $^3D_{CH}$) by selectively inverting a ^1H atom and reading the long-range couplings with ^{13}C atoms located two and three bonds away. Because this is an HSQC-based experiment, long-range couplings with quaternary carbon atoms are not observed. The extraction of the couplings is clean and straightforward, and in most cases gives the sign of the RDC values too. The experiment also gives accurate $^2J_{CH}$ and $^3J_{CH}$ values, adding a convenient new tool to the existing set of NMR experiments available for their measurement.[37] Addition of accurate long-range CH RDCs to the SVD fittings significantly improves the structural discrimination power in complex small molecules with multiple stereogenic centers. To date, the configurational and conformational analysis of complex small molecules in most laboratories is still performed using NOE interactions and ^3J analysis. However, once the short- and long-range homonuclear and heteronuclear connectivities are known, a set of one-bond and long-range RDCs often will suffice to unambiguously determine the 3D structure of these molecules.

Received: March 10, 2011
Revised: June 17, 2011
Published online: July 12, 2011

Keywords: configuration determination · *J* couplings · NMR spectroscopy · residual dipolar couplings · structure elucidation

[1] J. H. Prestegard, C. M. Bougault, A. I. Kishore, *Chem. Rev.* **2004**, *104*, 3519.
[2] G. Kummerlöwe, B. Crone, M. Kretschmer, S. F. Kirsch, B. Luy, *Angew. Chem.* **2011**, *123*, 2693; *Angew. Chem. Int. Ed.* **2011**, *50*, 2643.
[3] C. Aroulanda, V. Boucard, F. Guibé, J. Courtieu, D. Merlet, *Chem. Eur. J.* **2003**, *9*, 4536.
[4] J. L. Yan, A. D. Kline, H. P. Mo, M. J. Shapiro, E. R. Zartler, *J. Org. Chem.* **2003**, *68*, 1786.
[5] A. Mangoni, V. Esposito, A. Randazzo, *Chem. Commun.* **2003**, 154.
[6] J. C. Freudenberger, S. Knör, K. Kobzar, D. Heckmann, T. Paululat, H. Kessler, B. Luy, *Angew. Chem.* **2005**, *117*, 427; *Angew. Chem. Int. Ed.* **2005**, *44*, 423.
[7] C. M. Thiele, *J. Org. Chem.* **2004**, *69*, 7403.
[8] A. Schuetz, T. Murakami, N. Takada, J. Junker, M. Hashimoto, C. Griesinger, *Angew. Chem.* **2008**, *120*, 2062; *Angew. Chem. Int. Ed.* **2008**, *47*, 2032.
[9] C. M. Thiele, A. Marx, R. Berger, J. Fischer, M. Biel, A. Giannis, *Angew. Chem.* **2006**, *118*, 4566; *Angew. Chem. Int. Ed.* **2006**, *45*, 4455.
[10] C. M. Thiele, V. Schmidts, B. Böttcher, I. Louzao, R. Berger, A. Maliniak, B. Stevensson, *Angew. Chem.* **2009**, *121*, 6836; *Angew. Chem. Int. Ed.* **2009**, *48*, 6708.
[11] C. Gayathri, M. C. de la Fuente, B. Luy, R. R. Gil, A. Navarro-Vazquez, *Chem. Commun.* **2010**, *46*, 5879.

[12] P. Lesot, Y. Gounelle, D. Merlet, A. Loewenstein, J. Courtieu, *J. Phys. Chem.* **1995**, *99*, 14871.
[13] A. Marx, C. Thiele, *Chem. Eur. J.* **2009**, *15*, 254.
[14] C. M. Thiele, S. Berger, *Org. Lett.* **2003**, *5*, 705.
[15] G. Kummerlöwe, B. Luy, A. W. Graham, *Annu. Rep. NMR Spectrosc.* **2009**, *68*, 193.
[16] G. Kummerlöwe, E. F. McCord, S. F. Cheatham, S. Niss, R. W. Schnell, B. Luy, *Chem. Eur. J.* **2010**, *16*, 7087.
[17] C. Gayathri, N. V. Tsarevsky, R. R. Gil, *Chem. Eur. J.* **2010**, *16*, 3622.
[18] L. Verdier, P. Sakhaii, M. Zweckstetter, C. Griesinger, *J. Magn. Reson.* **2003**, *163*, 353.
[19] K. Kobzar, B. Luy, *J. Magn. Reson.* **2007**, *186*, 131.
[20] A. Bax, R. Freeman, *J. Am. Chem. Soc.* **1982**, *104*, 1099.
[21] L. Kay, P. Keifer, T. Saarinen, *J. Am. Chem. Soc.* **1992**, *114*, 10663.
[22] A. Bax, S. Subramanian, *J. Magn. Reson.* **1986**, *67*, 565.
[23] J. Schleucher, M. Schwendinger, M. Sattler, P. Schmidt, O. Schedletzky, S. J. Glaser, O. W. Sorensen, C. Griesinger, *J. Biomol. NMR* **1994**, *4*, 301.
[24] J. R. Tolman, J. H. Prestegard, *J. Magn. Reson. Ser. B* **1996**, *112*, 269.
[25] M. H. Levitt, R. Freeman, *J. Magn. Reson.* **1981**, *43*, 65.
[26] H. Schwalbe, P. Schmidt, C. Griesinger, *Coupling Constants Determined by ECOSY in Encyclopedia of Magnetic Resonance*, Wiley, Hoboken, **2007**.
[27] J. G. Blanco, R. R. Gil, C. I. Alvarez, L. C. Patrito, S. Genti-Raimondi, A. Flury, *FEBS Lett.* **1997**, *409*, 396.
[28] P. M. Dewick, *Nat. Prod. Rep.* **2002**, *19*, 181.
[29] K. E. Kövér, K. Feher, *J. Magn. Reson.* **2004**, *168*, 307.
[30] J. L. Marshall, *Methods in Stereochemical Analysis*, *Vol. 2*, Weinheim, Germany, **1983**.
[31] G. Kontaxis, G. M. Clore, A. Bax, *J. Magn. Reson.* **2000**, *143*, 184.
[32] J. A. Losonczi, M. Andrec, M. W. F. Fischer, J. H. Prestegard, *J. Magn. Reson.* **1999**, *138*, 334.
[33] MSpin. MESTRELAB RESEARCH SL, Santiago de Compostela, SPAIN. http://www.mestrelab.com.
[34] H. Schwalbe, P. Schmidt, C. Griesinger, in *Multidimensional NMR Methods for the Solution State*, Wiley, Hoboken **2010**, p. 177.
[35] E. E. Burnell, C. A. De Lange, *J. Magn. Reson.* **1980**, *39*, 461.
[36] G. Cornilescu, J. L. Marquardt, M. Ottiger, A. Bax, *J. Am. Chem. Soc.* **1998**, *120*, 6836.
[37] B. L. Marquez, W. H. Gerwick, R. T. Williamson, *Magn. Reson. Chem.* **2001**, *39*, 499.

